CHEMISTRY OF MATERIALS
Article

Chem. Mater. **2009,** *21,* 4839–4845 4839
DOI:10.1021/cm901322x

Nickel/Nickel Phosphide Core−Shell Structured Nanoparticles: Synthesis, Chemical, and Magnetic Architecture

Xianfeng Zheng, Songliu Yuan,* Zhaoming Tian, Shiyan Yin, Jinhua He, Kuili Liu, and Li Liu

School of Physics, Huazhong University of Science and Technology, Wuhan 430074, People's Republic of China

Received May 13, 2009. Revised Manuscript Received August 13, 2009

Discrete, magnetically recyclable, and oxidation-resistant nanoparticles with nickel/nickel phosphide core−shell structure were synthesized through surface-phosphatizing Ni nanoparticles using triphenylphosphine as the phosphorus source. The Ni_2P shell thickness was tunable by changing the reaction time in the mild temperature organic solution. And it was shown that the chemical architecture of core−shell can be useful to prepare Ni_3P nanogranular films through the chemical combination of Ni_2P shell with inner Ni during annealing. The core−shell magnetic architecture can also be helpful in improving the magnetically thermal stability through the effective influence of surface anisotropy after magnetic surface modification. The mechanism could be used to guide the synthesis and application of similar core−shell structured nanomaterials.

Introduction

The architecture with core and shell in nanomaterials has attracted considerable attention due to its valuable chemical property,[1] remarkable physical effect,[2] and also potential multifunctionality.[3] In particular, the core−shell architecture with chemical materials can provide new facile way, superior to conventional methods in preparing advanced nanomaterials.[4,5] And the core−shell architecture with magnet[6,7] or semiconduct[8,9] can bring novel effect through the interactions between core and shell. Moreover, the architecture containing bifunctional core and shell can lead multifunctionality deriving from the integration of various function into single nanoscale particle.[10,11] Solid-state Ni_2P is well-known as a corrosion-resistant and oxidation-resistant material. Significantly, nanosized Ni_2P particle is a new-found high-efficiency catalyst[12] for the hydrodesulfurization and hydrodenitrogenation procedure in environmental protection and petroleum refining,[13] and a potential n-type semiconductor[14] used for photoelectrochemical cell. A new type of nanoscale architecture consisting of a magnetic core and Ni_2P shell can be multifunctional, because it can provide a corrosion-resistant encapsulation[15,16] for the magnetic core used for magnetic separation in bioprocesses with oxygen or corrosives and can realize the magnetic separation and recycling[17] of multifunctional Ni_2P shell in applications. Furthermore, it is a magnetic metal-semiconductor[18,19] hybrid-nanostructure having potential properties from the interactions between the magnetic metal core and functional semiconductor shell.

Typically, the solid-state Ni_2P phase is obtained through direct solid phase combination of the elements at high temperatures. Recently, organic solution-phase technique has been developed to synthesize nanosized Ni_2P using trioctylphosphine[20,21] (TOP) as phosphorus

*Corresponding author. E-mail: yuansl@hust.edu.cn.

(1) Ge, J. P.; Zhang, Q.; Zhang, T. R.; Yin, Y. D. *Angew. Chem., Int. Ed.* **2008**, *47*, 8924.
(2) Zheng, H.; Wang, J.; Lofland, S. E.; Ma, Z.; Mohaddes-Ardabili, L.; Zhao, T.; Salamanca-Riba, L.; Shinde, S. R.; Ogale, S. B.; Bai, F.; Viehland, D.; Jia, Y.; Schlom, D. G.; Wuttig, M.; Roytburd, A.; Ramesh, R. *Science*. **2004**, *303*, 661.
(3) Zeng, H.; Sun, S. H. *Adv. Funct. Mater*. **2008**, *18*, 391.
(4) Teng, X. W.; Yang, H. *J. Am. Chem. Soc*. **2003**, *125*, 14559.
(5) Kim, J.; Rong, C. B.; Lee, Y. M.; Liu, J. P.; Sun, S. H. *Chem. Mater*. **2008**, *20*, 7242.
(6) Zeng, H.; Li, J.; Liu, J. P.; Wang, Z. L.; Sun, S. H. *Nature* **2002**, *420*, 395.
(7) Skumryev, V.; Stoyanov, S.; Zhang, Y.; Hadjipanayis, G.; Givord, D.; Nogues, J. *Nature* **2003**, *423*, 850.
(8) Thakar, R.; Chen, Y. C.; Snee, P. T. *Nano Lett*. **2007**, *7*, 3429.
(9) Chen, W. T.; Yang, T. T.; Hsu, Y. J. *Chem. Mater*. **2008**, *20*, 7204.
(10) Kim, H.; Achermann, M.; Balet, L. P.; Hollingsworth, J. A.; Klimov, V. I. *J. Am. Chem. Soc*. **2005**, *127*, 544.
(11) Ma, D. L.; Guan, J. W.; Normandin, F.; Denommee, S.; Enright, G.; Veres, T.; Simard, B. *Chem. Mater*. **2006**, *18*, 1920.
(12) Senevirathne, K.; Burns, A. W.; Bussell, M. E.; Brock, S. L. *Adv. Funct. Mater*. **2007**, *17*, 3933.
(13) Oyama, S. T. *J. Catal*. **2003**, *216*, 343.
(14) Panneerselvam, A.; Malik, M. A.; Afzaal, M.; O'Brien, P.; Helliwell, M. *J. Am. Chem. Soc*. **2008**, *130*, 2420.
(15) Zalich, M. A.; Vadala, M. L.; Riffle, J. S.; Saunders, M.; Pierre, T. G. S. *Chem. Mater*. **2007**, *19*, 6597.
(16) Chen, D.; Li, J. J.; Shi, C. S.; Du, X. W.; Zhao, N. Q; Sheng, J.; Liu, S. *Chem. Mater*. **2007**, *19*, 3399.
(17) Zhang, X. B.; Yan, J. M.; Han, S.; Shioyama, H.; Xu, Q. *J. Am. Chem. Soc*. **2009**, *131*, 2778.
(18) Casavola, M.; Grillo, V.; Carlino, E.; Giannini, C.; Gozzo, F.; Pinel, E. F.; Garcia, M. A.; Manna, L.; Cingolani, R.; Cozzoli, P. D. *Nano Lett*. **2007**, *7*, 1386.
(19) Lee, J. S.; Shevchenko, E. V.; Talapin, D. V. *J. Am. Chem. Soc*. **2008**, *130*, 9673.
(20) Chiang, R. K.; Chiang, R. T. *Inorg. Chem*. **2007**, *46*, 369.
(21) Henkes, A. E.; Schaak, R. E. *Chem. Mater*. **2007**, *19*, 4234.

Published on Web 09/22/2009

source. However, several nickel-based heterostructures by solution-phase synthesis were reported with Ni/NiO[22] or Ni/Ni_3C.[23] To the best of our knowledge, the Ni/Ni_2P core−shell architecture has never been reported before. In this article, we present a controllable synthesis of magnetically recyclable and oxidation-resistant nanoparticles with Ni/Ni_2P core−shell structure through surface-phosphatizing Ni nanoparticles using triphenylphosphine (TPP) as phosphorus source. And it is shown that the chemical architecture of core−shell can be useful to prepare Ni_3P nanogranular films through the chemical combination of Ni_2P shell with inner Ni during annealing. And the magnetic architecture can be helpful in improving the magnetically thermal stability through the effective influence of surface anisotropy after magnetically surface modification.

Experimental Section

Nickel(acetylacetonate)$_2$ [Ni(acac)$_2$, 99%, Aldrich], oleylamine (96%, Aldrich), triphenylphosphine (TPP, 99%, Aldrich), hexane, and ethanol were used as purchased without further purification. All preparation procedures were carried out under argon atmosphere using an argon-filled glovebox. The Ni/Ni_2P core−shell structured nanoparticles were chemically prepared by a mild temperature organic solution-phase reaction. In a typical synthesis technique, a mixture of oleylamine (38 g) and Ni(acac)$_2$ (1.8 g) was heated to 100 °C with magnetically stirring under an argon atmosphere, followed by injecting with TPP (12.6 g). The dark green solution was heated to 200 °C over 15 min and kept at this temperature for 30 min, giving Ni nanoparticles (Sample Ni) with average outer diameter about 25 nm (see Figure S1 in the Supporting Information). The resulting black solution was then quickly heated up to 280 °C and aged for 5 min (sample 1), 20 min (sample 2), and 90 min (sample 3), respectively. After cooling to room temperature naturally, excess ethanol was added to the black solution to give black precipitate, which was isolated via centrifugation, washed fully with ethanol, and dried under argon before being dispersed in hexane.

The mechanism for synthesizing Ni/Ni_2P nanoparticles can be depicted below. Ni−oleylamine complex[24] with TPP was decomposed at 200 °C to give large-sized Ni nanoparticles capped by surfactants containing TPP. Then the Ni nanoparticles were reacted with the attached TPP on the surface at 280 °C to make Ni_2P[25] shell with Ni remaining in the core. And the shell thickness was readily tuned by controlling the reaction time while keeping the other synthetic conditions fixed. Using large-sized Ni nanoparticles with diameter larger than 20 nm could lower the specific surface area in the reaction of Ni nanoparticles with attached TPP, and consequently make the insufficient and substoichiometric reaction possible.[22] Taking moderate reaction temperature of 280 °C could slow down the phosphatizing reaction of Ni nanoparticles, and accordingly make the structural evolvement controllable.[26] And this temperature with lower TPP concentrations could also reduce the rate contrast between outward-diffused Ni and inward-diffused P, to avoid the nanoscale voids formed in excessive TOP solution at higher temperature of 320 °C.[20] Herein, the TPP could serve as both surfactant and phosphorus source, and was used in our experiment in consideration of two facts: a stabilizing ligand consisting of three big phenyls whose particular molecular structure could give larger-sized Ni nanoparticles, and a phosphorus source having very low price compared with TOP.[24]

X-ray diffraction (XRD) patterns were obtained using a diffractometer (X'Pert PRO) equipped with a Cu Ka rotating anode source (λ = 0.1542 nm). The XRD samples were prepared by depositing hexane dispersion of the particles on a glass. Scanning electron microscope (SEM) images were taken with a field-emission scanning electron microscope (Model Sirion 200). Transmission electron microscopy (TEM) images were taken with a JEM-2010 transmission electron microscope operated at 200 kV. High-resolution transmission electron microscopy (HRTEM) images and energy-dispersive X-ray (EDX) analysis were obtained using a JEM-2010 field-emission analytical transmission electron microscope with an accelerating voltage of 200 kV. The TEM samples were prepared by dropping the hexane suspension onto a copper grid coated with carbon film before drying at room temperature under ambient conditions. Magnetic properties of fully washed particles were measured by a quantum design physical properties measurements system (PPMS) in the temperature range from 10 to 300 K and under the applied fields up to 2 T. To perform the zero-field-cooling (ZFC) measurement, the procedure was to cool the sample under zero applied field down to 10 K and then have an applied a field of 1 kOe for data collection in the warming process. For the field-cooling (FC) curve, the procedure was the same as that in the ZFC measurement, except that the sample was cooled with the presence of an applied magnetic field of 1 kOe.

Results and Discussion

Characterization of the Core−Shell Structure. The as-synthesized core−shell structured nanoparticles were characterized using XRD, TEM, HRTEM, and PPMS. High-magnification view of as-synthesized nanoparticles through TEM and their corresponding XRD patterns analysis are shown in Figure 1. For the TEM images in Figures 1a−c, the different contrast between the core and shell region results from the different electron penetration efficiency[27] on metallic Ni and phosphide Ni_2P. And it reveals that the shell thickness increased obviously from about 2−3 nm (Sample 1) to 5−6 nm (Sample 2) with the phosphatizing time increasing from 5 min (Sample 1) to 20 min (Sample 2). For the XRD patterns in Figure 1d, the added broad peaks[24,25] in the composite−structure pattern result from the nanoscale polycrystalline characteristic of hexagonal Ni_2P (JCPDS 74−1385) shell on the face-centered cubic (FCC) Ni (JCPDS 04−0850) core. And as the shell thickness increases, the diffraction from the Ni_2P shell shows more evidently in the patterns. Simultaneously, the inner Ni core reduces approximately from 20−22 nm (Sample 1) to 14−16 nm (Sample 2) in

(22) Lee, S.; Lee, N.; Park, J.; Kim, B. H.; Yi, Y. W.; Kim, T.; Kim, T. K.; Lee, I. H.; Paik, S. R.; Hyeon, T. *J. Am. Chem. Soc.* **2006**, *128*, 10658.
(23) Zhou, W.; Zheng, K.; He, L.; Wang, R. M.; Guo, L.; Chen, C. P.; Han, X. D.; Zhang, Z. *Nano Lett.* **2008**, *8*, 1147.
(24) Park, J.; Kang, E.; Son, S. U.; Park, H. M.; Lee, M. K.; Kim, J.; Kim, K. W.; Noh, H. J.; Park, J. H.; Bae, C. J.; Park, J. G.; Hyeon, T. *Adv. Mater.* **2005**, *17*, 429.
(25) Henkes, A. E.; Vasquez, Y.; Schaak, R. E. *J. Am. Chem. Soc.* **2007**, *129*, 1896.
(26) Yin, Y. D.; Erdonmez, C. K.; Cabot, A.; Hughes, S.; Alivisatos, A. P. *Adv. Funct. Mater.* **2006**, *17*, 1389.
(27) Zeng, H.; Li, J.; Wang, Z. L.; Liu, J. P.; Sun, S. H. *Nano Lett.* **2004**, *4*, 187.

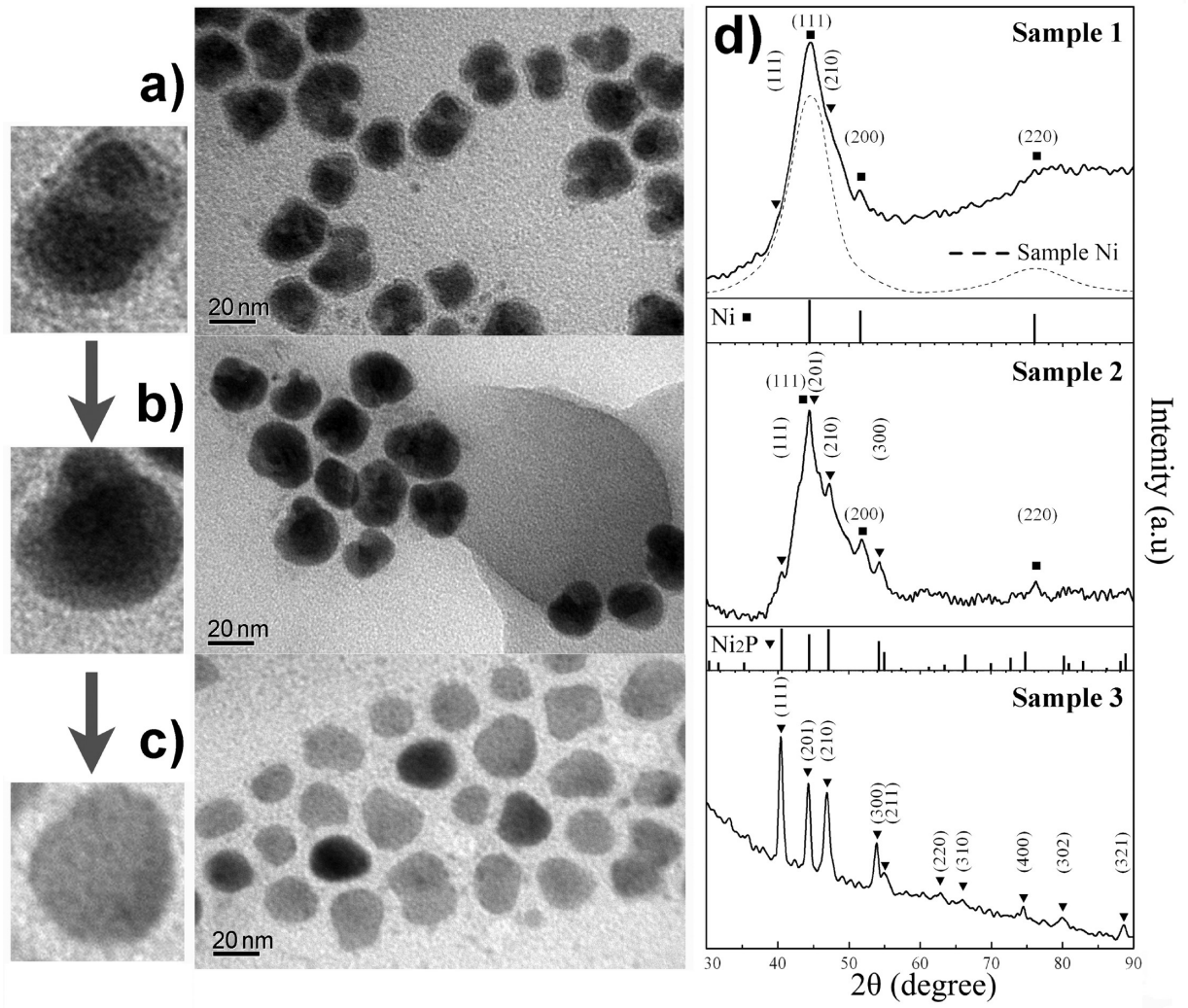

Figure 1. High-magnification TEM images of as-synthesized nanoparticles from (a) sample 1 phosphatized for 5 min, (b) sample 2 phosphatized for 20 min, and (c) sample 3 phosphatized for 90 min, and (d) corresponding XRD patterns.

diameter with the increase of Ni_2P shell thickness, because of the phosphatizing reaction consuming the inner Ni core. And the average size of the nanoparticles about 26 nm has not made a big change during the reaction. However, overphosphatizing the particles would make Ni_2P nanoparticles form with almost no Ni remaining. The average shell thickness can also be calculated from the reduction of saturation magnetization at room temperature, combined with TEM observation.[28] Assuming a spherical core−shell structure with an average outer diameter of 26 nm, the saturation magnetization value reduces from 3.8 emu/g (sample 1) to 1.6 emu/g (sample 2), which corresponds to the increased shell thickness of nonferromagnetic Ni_2P from 2.5 to 5.5 nm, which is reasonably consistent with the TEM observation.

The core−shell structure was further characterized at atomic scale using HRTEM as shown in Figure 2. A low-magnification HRTEM image from sample 2 shows the discrete nanoparticles with an average size of around 26 nm, as seen from the inset of Figure 2a. And the HRTEM image in Figure 2a shows a representative core−shell structured nanoparticle with a core about 14 nm in diameter surrounded by a shell about 6 nm in thickness.[29] Energy-dispersive X-ray (EDX) elemental analysis of it as shown in Figure 2b reveals that the shell layer contains both Ni and P with atom ratio 2:1 and the core contains mainly Ni (see Figure S2 in the Supporting Information). The HRTEM lattice image in Figure 2c shows the lattice fringes of the core with lattice distances of 1.76 Å corresponding to (200) lattice planes for FCC Ni, and the shell with adjacent fringe spacing of 1.92 Å corresponding to (210) planes for hexagonal Ni_2P, in agreement with the XRD data. And the fast Fourier transformation (FFT) pattern in the inset of Figure 2c showing the diffraction spots of marked lattice planes reveals the FCC Ni core surrounded by polycrystalline Ni_2P, indicating that the surface-phosphatizing reaction induced multiple nucleation sites of Ni_2P with altered crystallographic orientation to match the inner Ni lattice structure, for minimizing the lattice mismatch energy.

(28) Johnston-Peck, A. C.; Wang, J. W.; Tracy, J. B. *ACS Nano* **2009**, *3*, 1077.

(29) Li, J.; Zeng, H.; Sun, S. H.; Liu, J. P.; Wang, Z. L. *J. Phys. Chem. B* **2004**, *108*, 14005.

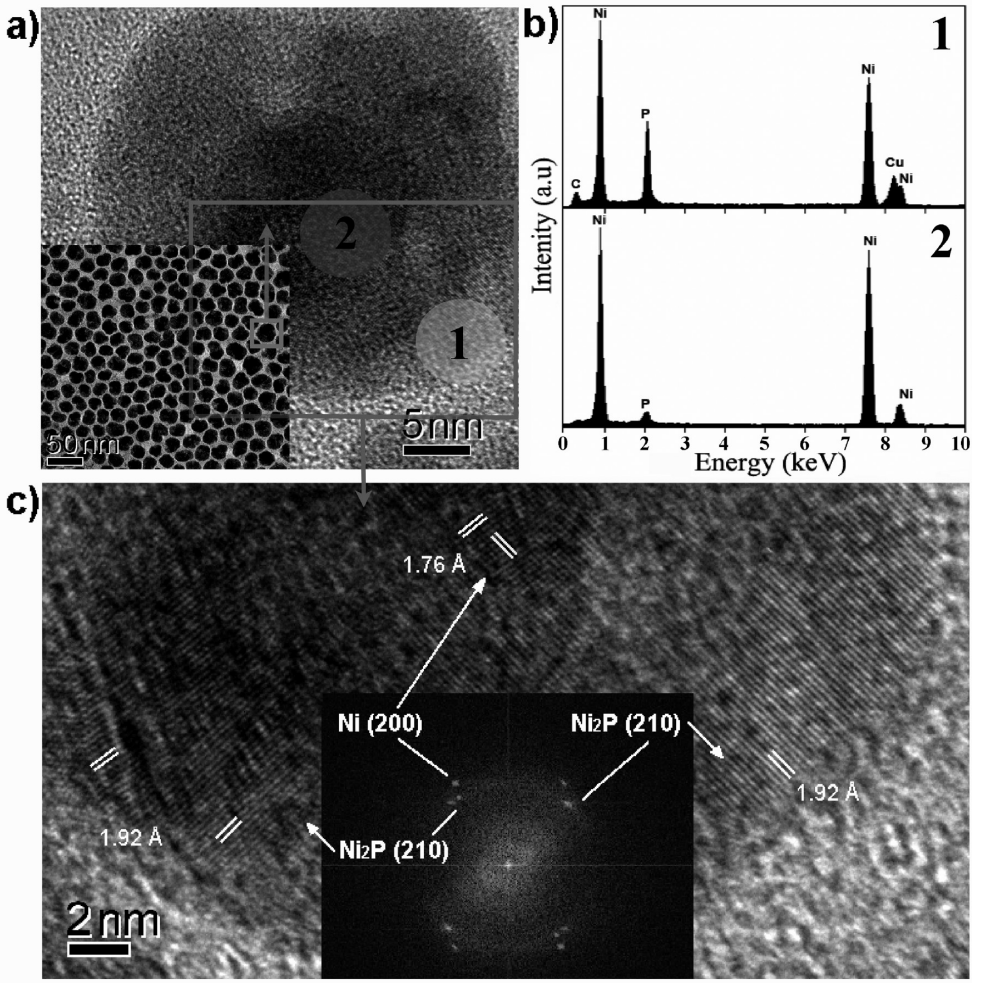

Figure 2. (a) HRTEM images of as-synthesized Ni/Ni_2P nanoparticles from sample 2 (inset) and a single Ni/Ni_2P core−shell structured nanoparticle. (b) EDX spectra acquired from the shell (1, top) and the core (2, bottom). (c) High-resolution lattice image and corresponding FFT pattern (inset) of the core and shell.

Core−Shell Chemical Architecture. On the one hand, as shown in Figure 3a the XRD pattern of sample 1 exposed to air in powder form for 1 month is similar to the patterns measured after synthesis (Figure 1). And no new diffraction peaks for possible oxides or hydroxides could be detected. The saturation magnetization value 3.8 emu/g also shows no change in the magnetization measurement at room temperature, which can be attributable to the chemical role of Ni_2P shell as oxidation-resistant encapsulation for inner Ni core. Thus, the Ni/Ni_2P core−shell structured nanoparticles are superior to the single-component Ni nanoparticles, which were readily oxidized to NiO after being exposed to air for only 1 day,[24] and can be used for magnetic separation in bioprocesses with oxygen or corrosives.

On the other hand, the XRD pattern of sample 1 after annealing at 600 °C under argon atmosphere reveals the formation of Ni_3P (JCPDS 74−1384) with remaining Ni phase as shown in Figure 3b. And after adjusting the core−shell proportion by reaction time, annealing sample 2 at 600 °C would lead the formation of Ni_3P nanogranular film with almost no Ni remaining as shown in Figure 4. By calculating from the average shell thickness with assuming a spherical 26 nm core−shell structure, the average molar ratio of Ni core to Ni_2P shell for sample 1 is approximately 3:1, and for sample 2 is 1:1. Thus, the formation of Ni_3P can be attributed to the chemical role of Ni_2P shell as precursors to chemically combine with inner Ni during annealing (Ni + Ni_2P → Ni_3P). For preparing Ni_3P granular films in our experiments, the Ni/Ni_2P nanoparticles were deposited and self-assembled on a corundum substrate by precipitating and drying the hexane suspension in vacuum, and then were annealed at 600 °C under argon atmosphere for one hour. Solid-state Ni_3P phase was usually prepared by reacting nickel with red phosphorus[30] at temperature as higher as 800 °C for a longer time, and was a new-found catalyst for gas phase hydrodechlorination.[31,32] Thus, the core−shell chemical architecture provides a new valuable method to realize the synthesis of Ni_3P nanogranular film at lower temperatures and a potential way to obtain discrete Ni_3P nanoparticles by annealing the Ni/Ni_2P nanoparticles with aggregation-resistant[33] materials.

Core−Shell Magnetic Architecture. As shown in Figure 5a, the temperature dependent magnetization

(30) Pfeiffer, H.; Tancret, F.; Brousse, T. *Mater. Chem. Phys.* **2005**, *92*, 534.
(31) Liu, X. G.; Chen, J. X; Zhang, J. Y. *Catal. Commun.* **2007**, *8*, 1905.
(32) Hu, X. L.; Yu, J. C. *Chem. Mater.* **2008**, *20*, 6743.
(33) Kim, J.; Rong, C. B.; Liu, J. P.; Sun, S. H. *Adv. Mater.* **2009**, *21*, 906.

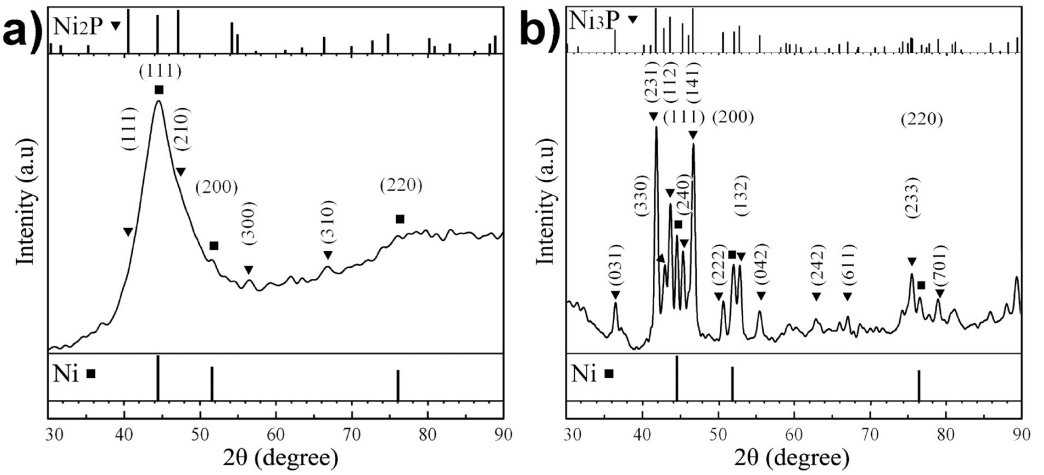

Figure 3. XRD patterns acquired from sample 1 (a) after exposing to air for 1 month and (b) after annealing at 600 °C under argon atmosphere for 1 h.

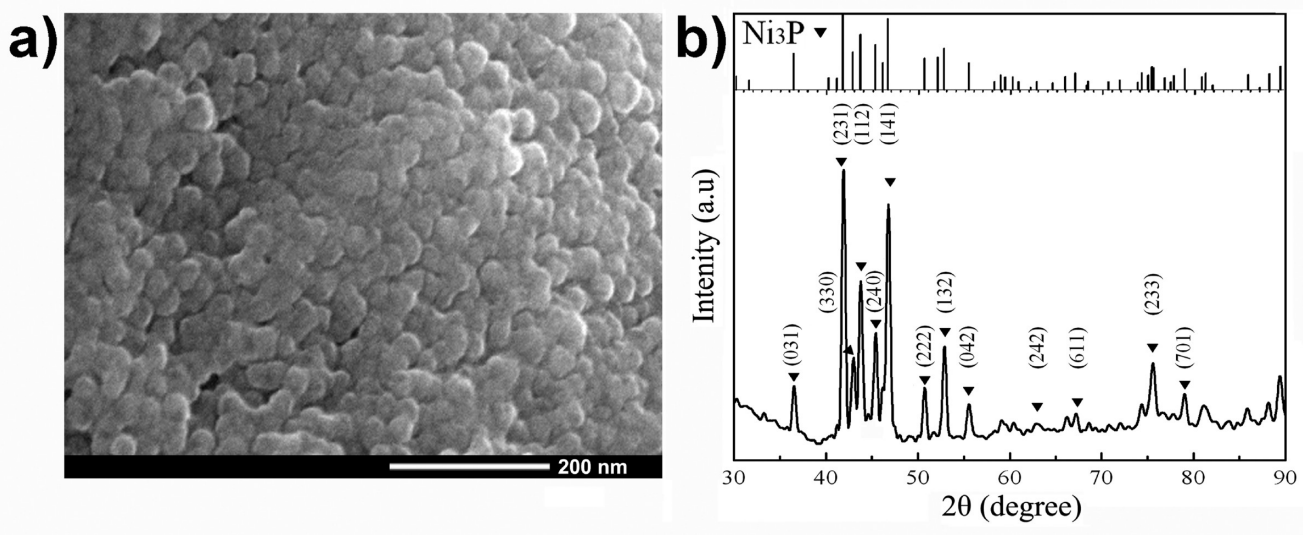

Figure 4. (a) SEM image and (b) corresponding XRD pattern of Ni_3P granular film acquired from annealing sample 2 at 600 °C under an argon atmosphere for 1 h.

curves of sample 1 reveal a divergence of the FC curve from ZFC curve with a peak. And the peak at 80 K corresponds to the average blocking temperature T_B, at which the magnetic anisotropy energy of nanoparticles responsible for holding the magnetic moment became comparable to the thermal energy.[7] The blocking temperature behavior is also confirmed by the field dependence of magnetization for sample 1 at different temperatures, as seen from the inset of Figure 5a. The magnetic hysteresis disappears at temperatures higher than the T_B, indicating that the thermal fluctuations induced random flipping of the magnetic moment with time and the nanoparticles exhibited transforming to superparamagnetism. For sample 2, similar transforming behavior is also seen from the field dependence of magnetization at varied temperatures (see Figure S3 in the Supporting Information). And the saturation magnetization (M_s) value of sample 2 is clearly smaller that of sample 1 at different temperatures, indicating the diminished Ni core of sample 2. Moreover, as seen from the inset of panels b and c in Figure 5 the magnetization of both samples at 10 K was not saturated even when the applied magnetic field reached 20 kOe. And the ZFC curve of sample 2 below T_B as shown in Figure 5b emerges a plateau and a similar climbing as that of Ni_2P nanoparticles in Figure 5c. It evidently demonstrated the presence of Ni_2P shell as magnetically surface modification layer for Ni core.

Normally, the T_B of single-component ferromagnetic nanoparticles decreases with diminishing size.[34] And the T_B of nanoparticles interacting through dipolar coupling should also decrease with increasing interparticle distance tuned by nonferromagnetic shell thickness.[35,36] Remarkably, the T_B of sample 2 with diminishing Ni core and rising interparticle distance increased to approximate 150 K as seen from Figure 5b. Consequently, the magnetic moments for the ferromagnetic core of sample

(34) Song, Q.; Zhang, Z. J. *J. Am. Chem. Soc.* **2004**, *126*, 6164.
(35) Frankamp, B. L.; Boal, A. K.; Tuominen, M. T.; Rotello, V. M. *J. Am. Chem. Soc.* **2005**, *127*, 9731.
(36) Yang, H. T.; Hasegawa, D.; Takahashi, M.; Ogawa, T. *Appl. Phys. Lett.* **2009**, *94*, 013103.

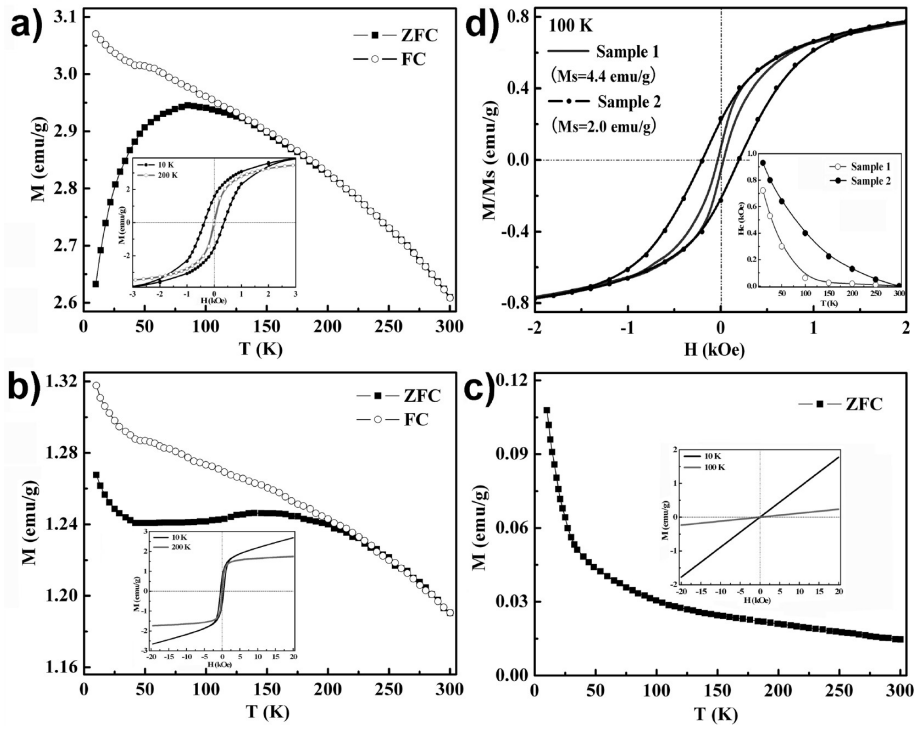

Figure 5. Magnetization under 1 kOe field as a function of temperature and as a function of field at different temperatures (inset), acquired from (a) sample 1 phosphatized for 5 min, (b) sample 2 phosphatized for 20 min, and (c) sample 3 phosphatized for 90 min. (d) Comparison of magnetic hysteresis loops from sample 1 and sample 2 at 100 K and their coercivities at varied temperatures (inset).

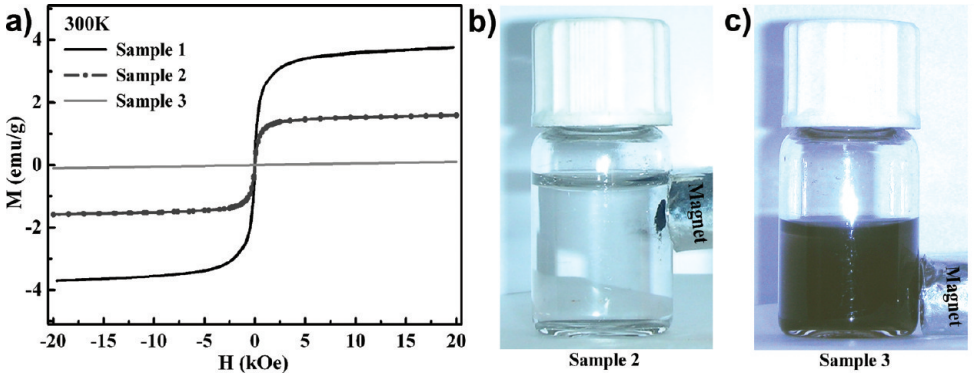

Figure 6. (a) Magnetic hysteresis loops of nanoparticles at room temperature, (b) picture showing magnetic attraction of Ni/Ni_2P nanoparticles from sample 2, and Ni_2P nanoparticles from sample 3.

2 were obviously more stable against thermal fluctuations, comparing with that of sample 1 at 100 K as shown in Figure 5d. And the coercivity (H_C) of sample 2 also remains larger than that of sample 1 at temperatures below 300 K, as seen from the inset of Figure 5d. It can be not described by a simply composite contribution of similar-sized ferromagnetic core and paramagnetic shell, indicating a magnetic coupling of core with modified surface. Taking into account that T_B is defined as $T_B = K_A V/25k_B$, where K_A is the magnetic anisotropy constant, V is the magnetic core volume, and k_B is the Boltzmann constant.[18] The K_A calculated from sample 1 is 5.8×10^3 J/m^3, and from sample 2 is 29×10^3 J/m^3. In fact, nickel is known to have relatively weak bulk magnetocrystalline anisotropy K_B (5×10^3 J/m^3),[16] which can allow a dominant contribution of surface anisotropy (K_S) to K_A (defined as $K_A = K_B + 6K_S/D$) for nanoparticles with enough reduced linear size D.[37,38] And effective K_S can originate from many different surface effects[39,40] and can be enhanced by any symmetry breaking at the surface, reduced interatomic exchange coupling at the interface, surface-core magnetostriction and strains, which can influence the spin configuration of the core via exchange coupling. Thus, the improved T_B can be attributed to the enhanced effective influence of the surface anisotropy with reduced magnetic core after magnetic surface modification.

(37) Garanin, D. A.; Kachkachi, H. *Phys. Rev. Lett.* **2003**, *90*, 065504.
(38) Biasi, E. D.; Zysler, R. D.; Ramos, C. A.; Romero, H.; Fiorani, D. *Phys. Rev. B* **2005**, *71*, 104408.
(39) Shi, W.; Zeng, H.; Sahoo, Y.; Ohulchanskyy, T. Y.; Ding, Y.; Wang, Z. L.; Swihart, M.; Prasad, P. N. *Nano Lett.* **2006**, *6*, 880.
(40) Salazar-Alvarez, G.; Qin, J.; Sepelak, V. S.; Bergmann, I.; Vasilakaki, M.; Trohidou, K. N.; Ardisson, J. D.; Macedo, W. A. A.; Mikhaylova, M.; Muhammed, M.; Baro, M. D.; Nogues, J. *J. Am. Chem. Soc.* **2008**, *130*, 13234.

The room-temperature magnetic hysteresis loops of as-synthesized nanoparticles as shown in Figure 6a reveal that nanoparticles from sample 2 exhibit a superparamagnetic behavior as that of sample 1 and a reduced saturation magnetization value of 1.6 emu/g comparing with 3.8 emu/g of sample 1, due to the reduced size of ferromagnetic core with increased nonferromagnetic shell thickness after phosphatizing reaction. Consequently, for sample 2 as shown in Figure 6b, the Ni/Ni_2P nanoparticles suspended in ethanol can be easily attracted and separated by using a magnet, and then can be redispersed by sonication (see Figure S4 in the Supporting Information). However, as shown in Figure 6c, the Ni_2P nanoparticles can not accomplish these because of the very faint magnetization at room temperature. Thus, the superparamagnetism of the Ni core can provide a facile way to realize the easy separation and recycling of functional Ni_2P nanoshell for its potential applications in solution. Further studies are being focused on the development of potential multifunctional applications deriving from the magnetic metal Ni core with functional semiconductor Ni_2P shell.

Conclusion

Ni/Ni_2P core−shell structured nanoparticles were synthesized, for the first time, through surface-phosphatizing Ni nanoparticles using TPP as phosphorus source in a mild temperature organic solution. And increasing phosphatizing time would lead to thickening of the Ni_2P shell, with the Ni core diminishing. The discrete Ni/Ni_2P nanoparticles exhibited oxidation-resistant and magnetically recyclable multifunctionality. Moreover, annealing the Ni/Ni_2P nanoparticles with adjusted core−shell proportions at 600 °C would lead to formation of the Ni_3P phase through the chemical combination of Ni_2P shell with inner Ni core, showing that the core−shell chemical architecture can be useful to prepare Ni_3P nanogranular films. And the T_B of samples after magnetic surface modification improved through the effective influence of surface anisotropy, showing that the core−shell magnetic architecture can be helpful in improving the magnetic thermal stability. Further studies can also be focused on various applications of the multifunction deriving from the magnetic metal Ni core with functional semiconductor Ni_2P shell.

Acknowledgment. This work was supported by National 973 Project of China (Greant 2006CB921606) and by the Foundation from the Ministry of National Education (Greant 20060487011).

Supporting Information Available: TEM image of as-prepared Ni nanoparticles (Figure S1), HRTEM images of as-synthesized Ni/Ni_2P nanoparticles (Figure S2), field-dependent magnetization curves of samples (Figure S3), and magnetic separation and redispersion process (Figure S4) (PDF). This material is available free of charge via the Internet at http://pubs.acs.org.